ORGANOMETALLICS

pubs.acs.org/Organometallics Article

Nickel(II)–Nickel(II) Azadithiolates: Synthesis, Structural Characterization, and Electrocatalytic H_2 Production

Li-Cheng Song,* Wen-Bo Liu, and Bei-Bei Liu

Cite This: https://dx.doi.org/10.1021/acs.organomet.0c00130 Read Online

ACCESS | Metrics & More | Article Recommendations | Supporting Information

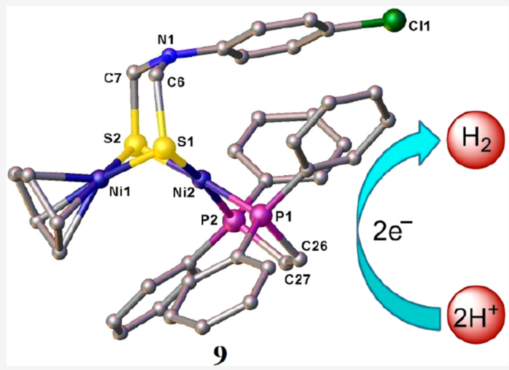

ABSTRACT: Azadithiolato-bridged dinuclear Ni_2 complexes with the general formula $[(\eta^5\text{-}C_5H_5)Ni\{(\mu\text{-}SCH_2)_2NC_6H_4R\text{-}4\}Ni(diphos)]BF_4$ (**8–11**, R = H, Cl, MeO; diphos = dppv, dppe) have been prepared by a well-designed synthetic method including the following three separate reaction steps. The first reaction step involves preparation of the bis(thioester) precursors 4-$RC_6H_4N(CH_2S\text{-}(O)CMe)_2$ (**1–3**, R = H, Cl, MeO) by a cocondensation reaction of aniline or its substituted derivatives 4-$RC_6H_4NH_2$ with 37% aqueous formaldehyde and thioacetic acid. The second step involves preparation of the mononuclear Ni precursors (diphos)$Ni[(SCH_2)_2NC_6H_4R\text{-}4]$ (**4–7**, R = H, Cl, MeO; diphos = dppv, dppe) by a one-pot reaction of bis(thioester) precursors **1–3** with *t*-BuONa followed by treatment of the resulting disodium intermediates 4-$RC_6H_4N(CH_2SNa)_2$ with (dppv)$NiCl_2$ and (dppe)$NiCl_2$, respectively. The third step involves preparation of the targeted dinuclear Ni_2 complexes **8–11** by coordination reactions of mononuclear Ni precursors **4–7** with $[\eta^5\text{-}C_5H_5Ni]^+$ generated in situ from dissociation of the triple-decker sandwich complex $[(C_5H_5)_3Ni_2]BF_4$. While all of the prepared compounds **1–11** have been characterized by elemental analysis and various spectroscopic techniques, the molecular structures of precursor complex **5** and targeted complexes **9** and **11** have been further confirmed by X-ray crystallography. In addition, the two representative targeted complexes **8** and **9** have been found to be catalysts for proton reduction to hydrogen using acetic acid as the proton source under electrochemical conditions.

■ INTRODUCTION

Hydrogenases (H_2ases) constitute a class of metalloenzymes that catalyze H_2 metabolism in a variety of microbes such as bacteria, archaea, and some eukaryotes.[1,2] According to the metal composition in their active sites, H_2ases are usually divided into three major groups: [NiFe]-H_2ases,[3−5] [FeFe]-H_2ases,[6−8] and [Fe]-H_2ase.[9−11] An X-ray crystallographic study demonstrated that the active site of [NiFe]-H_2ases includes two metal centers, in which the Ni center is coordinated by two terminal cysteinato ligands, the Fe center is coordinated by one terminal CO and two terminal cyanide ligands, and the two metal centers are bound together by two bridging cysteinato ligands (Figure 1a).[12−14]

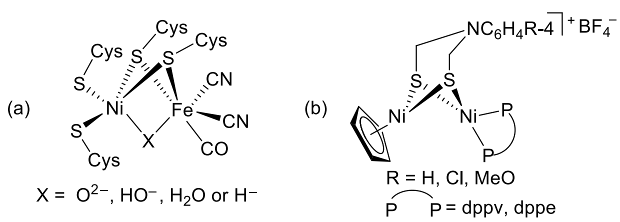

Figure 1. (a) Active site of [NiFe]-H_2ases. (b) Targeted dinuclear Ni_2 complexes.

Inspired by the well-elucidated structure shown in Figure 1a, synthetic chemists have prepared a large number of the hetero- and homodinuclear Ni–M (M = Fe, Ru, Mn, Mo, W, Co, Ni, etc.)-based biomimetic mimics for [NiFe]-H_2ases, but none of them contain the azadithiolato type of ligand.[15−43] Recently, considering that the bridging azadithiolato ligand in the active site of [FeFe]-H_2ases can play a key role in the catalytic redox reaction between H_2 and protons[44−46] and in order to further develop the biomimetic chemistry of [NiFe]-H_2ases, we decided to prepare the first azadithiolato ligand containing dinuclear Ni_2 complexes in which each of the azadithiolato 4-$RC_6H_4N(CH_2S)_2$ ligands is bridged between the two Ni atoms in CpNi and (diphosphine)Ni moieties (Figure 1b). Fortunately, we have successfully synthesized and structurally characterized such a type of dinuclear Ni_2 complex and in particular some of them have been found to be catalysts for

Received: February 22, 2020

proton reduction to H_2 under CV conditions. Herein, we report the interesting results obtained in this study.

■ RESULTS AND DISCUSSION

Synthesis and Characterization of the *N,N*-Bis(acetylthiomethyl)-Containing Compounds 4-RC_6H_4N-$[CH_2S(O)CMe]_2$ (1, R = H; 2, R = Cl; 3, R = MeO). According to our designed synthetic method for the preparation of the first azadithiolato-bridged dinuclear Ni_2 complexes, we should first prepare the two types of precursors. The first types of precursors are the *N,N*-bis(acetylthiomethyl)-containing benzene derivatives **1**−**3**, which could be prepared in 75−81% yields by a cocondensation reaction of aniline or its 4-substituted derivatives 4-$RC_6H_4NH_2$ with 37% aqueous formaldedyde and thioacetic acid in EtOH solvent (Scheme 1).

Scheme 1. Synthesis of Bis(thioester) Precursors 1−3

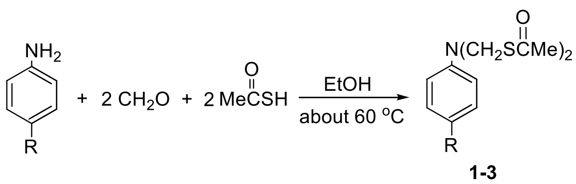

While the precursor compound **2** is known,[47] compounds **1** and **3** are new. **1**−**3** are all air-stable white solids and were characterized by elemental analysis and various spectroscopic methods. For example, the IR spectra of **1**−**3** showed one strong absorption band at ca. 1689 cm^{-1} for their thioester carbonyls. The ^1H NMR spectra displayed two singlets at ca. 2.37 and 5.08 ppm for the $CH_3C{=}O$ and CH_2 groups in their *N,N*-bis(acetylthiomethyl) substituents, respectively. The $^{13}C\{^1H\}$ NMR spectra exhibited one singlet at ca. 196 ppm for the thioester carbonyl C atoms.

Synthesis and Characterization of the Azadithiolato-Chelated Mononuclear Ni Complexes (dppv)Ni-$[(SCH_2)_2NC_6H_4R$-4] (4, R = H; 5, R = Cl) and (dppe)Ni-$[(SCH_2)_2NC_6H_4R$-4] (6, R = H; 7, R = MeO). The second types of precursors used for preparing the targeted dinuclear Ni_2 azadithiolates are the azadithiolato ligand chelated mononuclear Ni complexes **4**−**7**, which were prepared by a MeCO/Na exchange reaction of the first types of precursors **1**−**3** with *tert*-butoxysodium in THF from −78 °C to room temperature followed by a salt elimination reaction of the resulting disodium intermediates 4-$RC_6H_4N(CH_2SNa)_2$[48] with $(dppv)NiCl_2$ or $(dppe)NiCl_2$ in 41−49% yields, respectively (Scheme 2).

The new precursor complexes **4**−**7** are air-stable red solids and were also characterized by elemental analysis and various spectroscopic techniques. For instance, the ^1H NMR spectra of **4**−**7** displayed one singlet in the region 4.44−4.50 ppm for the two CH_2 groups in the azadithiolato ligands. The $^{13}C\{^1H\}$ NMR spectra showed one singlet in the range 47.4−48.3 ppm for the two C atoms in the two methylene groups, whereas the $^{31}P\{^1H\}$ NMR spectra displayed one singlet at ca. 63 and 57 ppm for the two P atoms in the dppv and dppe ligands, respectively.

The molecular structure of complex **5** was successfully determined by X-ray crystal diffraction analysis (Figure 2 and Table 1). As shown in Figure 2, complex **5** is an azadithiolato 4-$ClC_6H_4N(CH_2S)_2$ and a diphosphine dppv chelated mononuclear Ni complex. While the dppv ligand is chelated via its P1 and P2 atoms to the Ni1 atom to constitute an envelope-shaped five-membered metallacycle, the azadithiolato ligand is chelated via its S1 and S2 atoms to the Ni1 atom to construct a boat-shaped six-membered metallacycle that is axially attached to the 4-chlorophenyl group via the N1 atom. The bond lengths Ni1−P1 (2.1689 Å), Ni1−P2 (2.1467 Å), Ni1−S1 (2.1810 Å), and Ni1−S2 (2.1865 Å) in **5** are close to those corresponding to the previously reported analogue $(dppe)Ni(SCH_2)_2NC_6H_4Cl$-4.[48] The dihedral angle between the two planes P1Ni1P2 and S1Ni1S2 in **5** is equal to 0.394°, implying that the Ni1 atom adopts an ideal square-planar

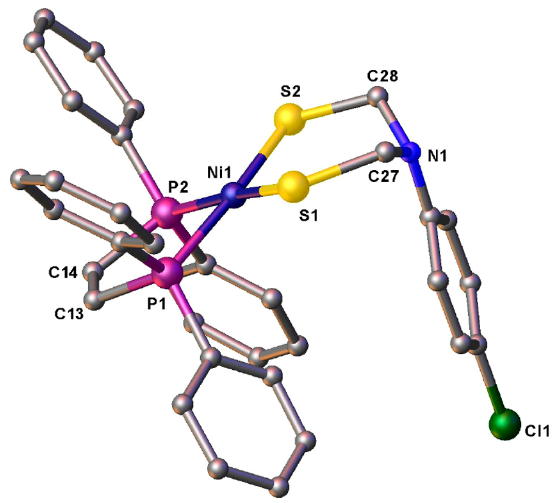

Figure 2. Molecular structure of **5** with ellipsoids drawn at the 50% probability level. All hydrogen atoms are omitted for the sake of clarity.

Scheme 2. Synthesis of Mononuclear Ni Precursors 4−7

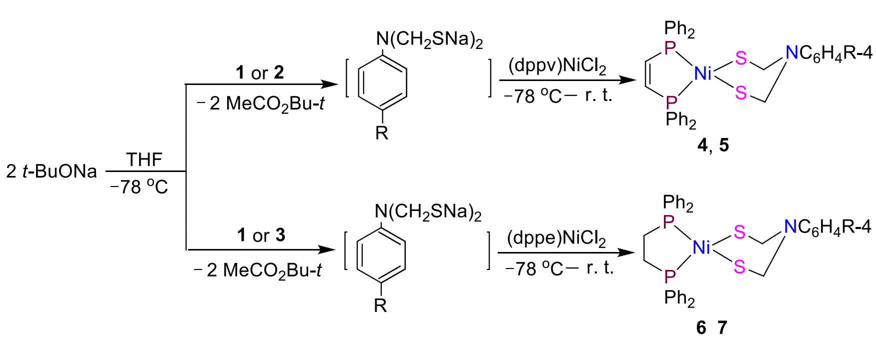

https://dx.doi.org/10.1021/acs.organomet.0c00130
Organometallics XXXX, XXX, XXX−XXX

Table 1. Selected Bond Lengths (Å) and Angles (deg) for 5

Ni(1)–S(1)	2.1810(9)	N(1)–C(27)	1.431(5)
Ni(1)–S(2)	2.1865(8)	N(1)–C(28)	1.447(4)
Ni(1)–P(1)	2.1689(9)	P(1)–C(13)	1.811(3)
Ni(1)–P(2)	2.1467(10)	P(2)–C(14)	1.823(3)
S(1)–Ni(1)–S(2)	102.67(3)	C(27)–N(1)–C(28)	113.1(3)
P(1)–Ni(1)–P(2)	87.31(3)	C(13)–P(1)–Ni(1)	108.94(11)
P(1)–Ni(1)–S(1)	85.80(3)	C(14)–P(2)–Ni(1)	108.81(12)
P(1)–Ni(1)–S(2)	171.53(4)	C(27)–S(1)–Ni(1)	111.41(12)

geometry. However, in contrast to this, the corresponding dihydral angle in the previously reported analogue (dppe)Ni-$(SCH_2)_2NC_6H_4Cl$-4 is 27.6°,[48] which implies that its Ni1 atom is best described as having a distorted-square-planar geometry.

Synthesis and Characterization of the Azadithiolato-Bridged Dinuclear Ni_2 Complexes $[(\eta^5\text{-}C_5H_5)Ni\{(\mu\text{-}SCH_2)_2NC_6H_4R\text{-}4\}Ni(dppv)]BF_4$ (8, R = H; 9, R = Cl) and $[(\eta^5\text{-}C_5H_5)Ni\{(\mu\text{-}SCH_2)_2NC_6H_4R\text{-}4\}Ni(dppe)]BF_4$ (10, R = H; 11, R = MeO). Particularly interesting is that the targeted azadithiolato ligand-bridged dinuclear Ni_2 complexes could be prepared by a coordination reaction of the second types of precursors **4**–**7** with the in situ generated cation $[\eta^5\text{-}C_5H_5Ni]^+$ from dissociation of the triple-decker sandwich complex $[(C_5H_5)_3Ni_2]BF_4$[49] in nitromethane at room temperature in 69–92% yields (Scheme 3).

Scheme 3. Synthesis of Targeted Dinuclear Ni_2 Complexes 8–11

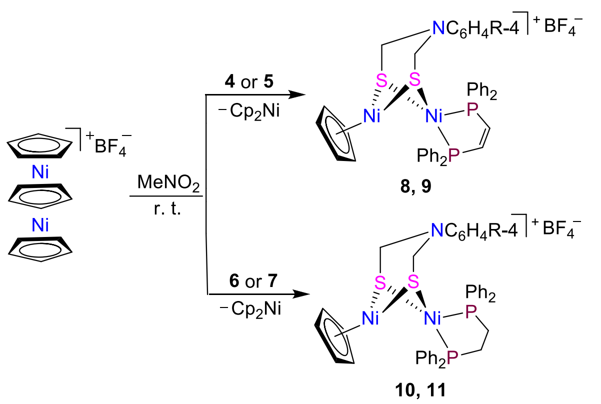

Dinuclear Ni_2 complexes **8**–**11** are air-stable brown solids. Their elemental analysis and spectral data are in good agreement with their structures shown in Scheme 3. For instance, the ^1H NMR spectra of **8**–**11** displayed one singlet in the range 4.81–5.12 ppm for the five H atoms in the Cp rings and two doublets in the range 4.12–4.52 ppm for the four H atoms in their azadithiolato methylene groups. The $^{13}C\{^1H\}$ NMR spectra exhibited one singlet at ca. 92 ppm for the five C atoms in the Cp rings, whereas the $^{31}P\{^1H\}$ NMR spectra displayed one singlet at about 70 and 60 ppm for the two P atoms in the dppv and dppe ligands, respectively.

The molecular structures of complexes **9** and **11** were unambiguously confirmed by an X-ray crystallographic study (Figures 3 and 4 and Table 2). As shown in Figures 3 and 4, both **9** and **11** are monocationic dinuclear Ni_2 complexes, each containing one monocation $[CpNi\{(\mu\text{-}SCH_2)_2NC_6H_4Cl\text{-}4\}\text{-}Ni(dppv)]^+$ or $[CpNi\{(\mu\text{-}SCH_2)_2NC_6H_4OMe\text{-}4\}Ni(dppe)]^+$ and one monoanion BF_4^-. In the two monocations, the

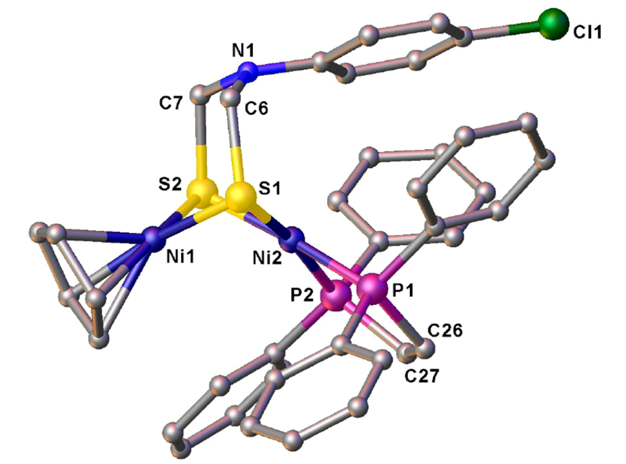

Figure 3. Molecular structure of **9** with ellipsoids drawn at the 50% probability level. All hydrogen atoms and the anion BF_4^- are omitted for the sake of clarity.

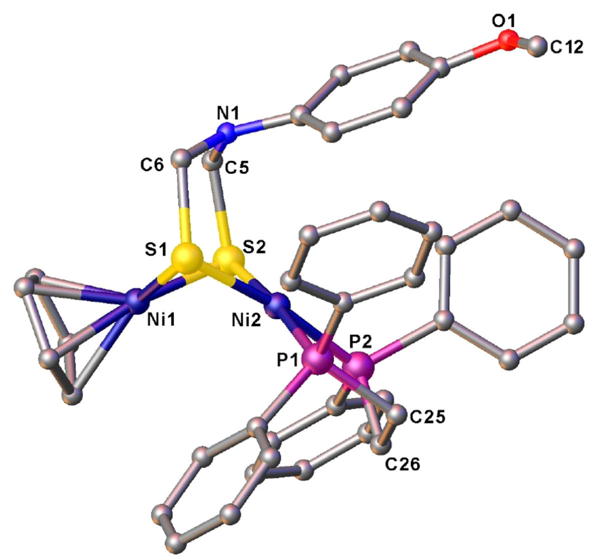

Figure 4. Molecular structure of **11** with ellipsoids drawn at the 50% probability level. All hydrogen atoms and the anion BF_4^- are omitted for the sake of clarity.

azadithiolato ligand 4-$ClC_6H_4N(CH_2S)_2$ in **9** or 4-$MeOC_6H_4N(CH_2S)_2$ in **11** is bridged to the Ni1 and Ni2 atoms to construct two fused six-membered metallacycles. While the metallacycle Ni1S1C6N1C7S2 in **9** adopts a chair conformation and another metallacycle Ni2S1C6N1C7S2 adopts a boat conformation, the metallacycle Ni1S1C6N1C5S2 in **11** takes a chair conformation and another metallacycle Ni2S1C6N1C5S2 takes a boat con-

https://dx.doi.org/10.1021/acs.organomet.0c00130
Organometallics XXXX, XXX, XXX–XXX

Table 2. Selected Bond Lengths (Å) and Angles (deg) for 9 and 11

Complex 9			
Ni(1)−S(1)	2.1825(16)	Ni(2)−P(1)	2.1446(16)
Ni(1)−S(2)	2.1893(15)	Ni(2)−P(2)	2.1651(15)
Ni(2)−S(1)	2.2123(15)	N(1)−C(6)	1.433(6)
Ni(2)−S(2)	2.2086(15)	P(1)−C(26)	1.814(5)
S(1)−Ni(1)−S(2)	89.05(6)	P(1)−Ni(2)−P(2)	88.26(6)
S(1)−Ni(2)−S(2)	87.80(5)	Ni(1)−S(1)−C(6)	102.1(2)
P(1)−Ni(2)−S(1)	89.24(6)	C(6)−N(1)−C(7)	113.1(5)
P(1)−Ni(2)−S(2)	175.34(6)	Ni(2)−P(1)−C(26)	108.66(19)
Complex 11			
Ni(1)−S(1)	2.1914(13)	Ni(2)−P(1)	2.1792(14)
Ni(1)−S(2)	2.1985(14)	Ni(2)−P(2)	2.1752(12)
Ni(2)−S(1)	2.1986(12)	N(1)−C(5)	1.423(6)
Ni(2)−S(2)	2.2111(13)	P(1)−C(25)	1.844(4)
S(1)−Ni(1)−S(2)	88.92(5)	P(1)−Ni(2)−P(2)	86.82(5)
S(1)−Ni(2)−S(2)	88.42(5)	Ni(1)−S(1)−Ni(2)	75.54(4)
P(1)−Ni(2)−S(1)	90.75(5)	C(5)−N(1)−C(6)	115.4(4)
P(1)−Ni(2)−S(2)	174.38(5)	Ni(2)−P(1)−C(25)	108.65(16)

formation. The 4-ClC_6H_4 group in **9** and 4-$MeOC_6H_4$ group in **11** are both bound to the common N1 atom of the corresponding two fused six-membered rings with an axial type of bond. It should be noted that (i) the Ni1−Ni2 distances of **9** (2.6781 Å) and **11** (2.6889 Å) are well beyond the sum of covalent radii of their two Ni atoms (1.24 Å + 1.24 Å = 2.48 Å),[50] which implies that no metal−metal bonding exists between their Ni1 and Ni2 atoms, and (ii) the two Ni1−Ni2 distances in **9** and **11** are much shorter than those of the reported 1,3-propanedithiolato ligand bridged dinuclear Ni_2 analogues $Cp_2Ni_2(\mu\text{-pdt})$ (2.863 Å).[35] and $[(dppe)_2Ni_2(\mu\text{-pdt})](BF_4)_2$ (2.871 Å).[51]

Electrochemical Properties and Electrocatalytic H_2-Producing Ability of Dinuclear Ni_2 Complexes 8 and 9. To date, a variety of homodinuclear Ni_2 complexes have been synthesized and some of them have been found to be electrocatalytic H_2-producing catalysts.[51−56] Having prepared the targeted dinuclear complexes **8**−**11**, we chose complexes **8** and **9** as representatives (due to **8** and **9** having the same types of structures as those of **10** and **11**) to study their electrochemical properties and electrocatalytic H_2-producing ability. The electrochemical properties of **8** and **9** were determined by cyclic voltammetric (CV) techniques by using n-Bu_4NPF_6 as the supporting electrolyte in MeCN at a scan rate of 100 mV s^{-1}. As shown in Table 3 and Figure 5, complexes **8** and **9** display one quasi-reversible reduction wave at −1.36 and −1.34 V, one irreversible reduction wave at −1.74 and −1.72 V, and one irreversible oxidation wave at 0.18 and 0.20 V, respectively. Similar to the previously reported cases,[51,52,57] the oxidation events of **8** and **9** each are one-electron processes, which was confirmed by bulk electrolysis of

Table 3. Electrochemical Data of 8 and 9[a]

compound	E_{pc1}/V	E_{pc2}/V	E_{pa}/V
8	−1.36	−1.74	0.18
9	−1.34	−1.72	0.20

[a]All potentials are versus Fc/Fc^+ in 0.1 M n-Bu_4NPF_6/MeCN at a scan rate of 0.1 V s^{-1}.

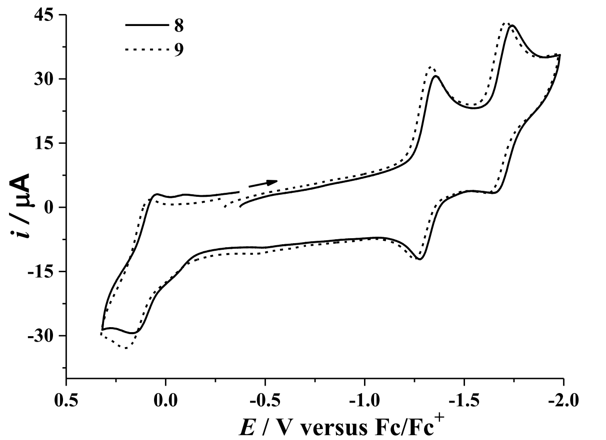

Figure 5. Cyclic voltammograms of **8** and **9** (1.0 mM) in 0.1 M n-Bu_4NPF_6/MeCN at a scan rate of 0.1 V s^{-1}. Arrows indicate the starting potential and scan direction.

a MeCN solution of **8** at 0.18 V (1.01 F mol^{-1} passed in 1 h) or **9** at 0.20 V (1.08 F mol^{-1} passed in 1 h). The reduction events displayed by **8** and **9** each are also one-electron processes, since their reduction peak current heights are close to their oxidation peak current heights. While the first reduction events of **8** and **9** could be assigned to the $CpNi^{II}Ni^{II}(dppv)/CpNi^{I}Ni^{II}(dppv)$ couple due to the $CpNi^{II}$ moieties in **8** and **9** each bearing a positive charge, the second reduction events of **8** and **9** could be attributed to the $CpNi^{I}Ni^{II}(dppv)/CpNi^{I}Ni^{I}(dppv)$ couple since the second reduction potentials of **8** and **9** are positively shifted relative to those displayed by their precursors **4** (−1.94 V) and **5** (−1.91 V) (see Figure S1) and in turn the oxidation events of **8** and **9** might be ascribed to the $CpNi^{II}Ni^{II}(dppv)/CpNi^{II}Ni^{III}(dppv)$ couple.[51,52,57] It should be noted that all of the reduction and oxidation waves of complex **9** are positively shifted by 20 mV relative to those of complex **8**, which is consistent with 4-ClC_6H_4 group in **9** being an electron-withdrawing group stronger than the C_6H_5 group in **8**. Additionally, the two reduction processes of **8** and **9** are all diffusion-controlled, since their reduction peak currents versus the square root of the scan rates (25−2000 mV s^{-1}) are linearly correlated (see Figures S2 and S3).[58]

To examine if complexes **8** and **9** could have the electrocatalytic ability for proton reduction to H_2, we further determined their cyclic voltammograms in the presence and absence (for comparison) of the weak acid HOAc (pK_a^{MeCN} = 22.3, $E°_{HA}$ = 1.35 V).[59,60] As shown in Figures 6 and 7, when 1−20 mM HOAc is sequentially added to MeCN solutions of **8** and **9**, the current heights of their original first reduction waves remain unchanged. However, in contrast to this, when 1−20 mM HOAc is sequentially added, the current heights of their original second reduction waves are considerably increased. Apparently, such an observation features an electrocatalytic process for proton reduction to hydrogen.[52,61,62] Furthermore, as shown in Figures 6 and 7, when 1−8 mM HOAc is continuously added, the original second reduction waves are positively shifted by about 40 mV, which is most likely caused by protonation of the central N atoms in their bridged azadithiolato ligands.[63]

In order to evaluate the electrocatalytic ability of **8** and **9**, we determined the ratio of the catalytic current (i_{cat}) to reductive peak current (i_p) in the absence of the added acid (note that a higher i_{cat}/i_p value means a faster catalysis).[62,64,65] At a

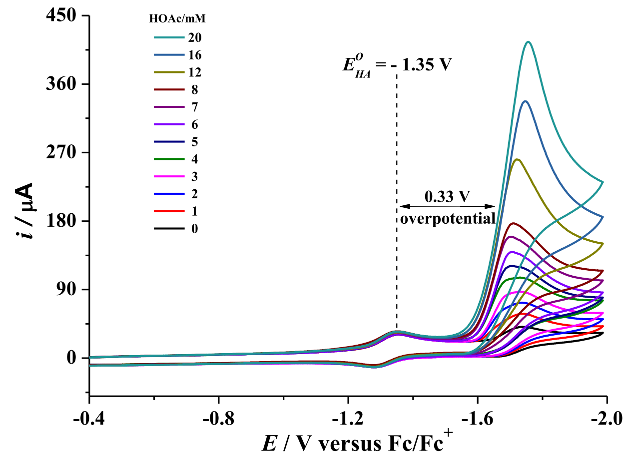

Figure 6. Cyclic voltammograms of **8** (1.0 mM) with HOAc (0−20 mM) in 0.1 M n-Bu_4NPF_6/MeCN at a scan rate of 0.1 V s^{-1}.

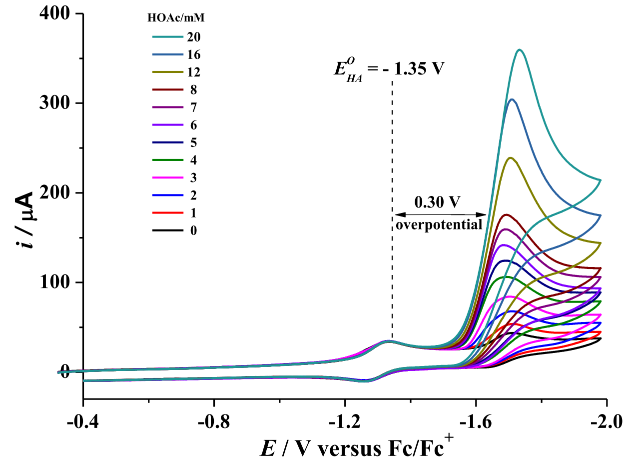

Figure 7. Cyclic voltammograms of **9** (1.0 mM) with HOAc (0−20 mM) in 0.1 M n-Bu_4NPF_6/MeCN at a scan rate of 0.1 V s^{-1}.

concentration of 20 mM HOAc, the i_{cat}/i_p values for **8** and **9** were calculated to be 20.3 and 18.2, respectively. It follows that the i_{cat}/i_p values of the azadithiolato-bridged dinuclear Ni_2 complexes **8** and **9** are much higher than those (7.8−12.2) of the previously reported dithiolato-bridged dinuclear complexes $Cp_2Ni_2(\mu$-$SR)_2$ (R = $PhCH_2$, C_8H_{17}, C_6H_4Me).[52] In addition, considering that overpotential (defined as the difference between the potential at the half-maximum of the catalytic current and the standard potential $E°_{HA}$ of the acid) is also an important parameter for evaluating the electrocatalytic ability for a catalyst (note that a better catalyst has a lower overpotential),[66,67] we further determined the overpotentials of **8** and **9** by using the Evans method.[59] At a concentration of 20 mM HOAc, the overpotentials of **8** and **9** were calculated to be 0.33 and 0.30 V, respectively (see Figures 6 and 7). It follows that the overpotentials of the azadithiolato-bridged dinuclear Ni_2 complexes **8** and **9** are much lower than those (0.57−0.61 V) of the previously reported dithiolato-bridged dinuclear Ni_2 complexes.[52]

Finally, it should be indicated that the electrocatalytic H_2 production catalyzed by **8** and **9** was proved by electrolysis of a MeCN solution of **8** or **9** (1.0 mM) with an excess amount of HOAc (50 mM) at −1.90 V. During 1 h of electrolysis, totals of 19.0 and 19.4 F mol^{-1} passed through the electrolysis cell, respectively; this corresponds to theoretical turnover numbers (TONs) of 9.5 and 9.7, respectively. Analysis by gas chromatography (GC) showed that the yields of H_2 evolved during the bulk electrolysis catalyzed by **8** and **9** are all above 90%.

■ SUMMARY AND CONCLUSIONS

On the basis of preparation of the bis(thioester) precursors **1**−**3** and mononuclear Ni precursors **4**−**7**, the first azadithiolato-bridged dinuclear Ni_2 complexes **8**−**11** have been synthesized by a coordination reaction of mononuclear Ni complexes **4**−**7** with the monocation $CpNi^+$ generated in situ from the triple-decker sandwich complex $(Cp_3Ni_2)BF_4$. The spectroscopic characterization of all the targeted complexes **8**−**11** and the X-ray crystallographic characterization of their two representatives **9** and **11** have proved that they all contain one azadithiolato ligand 4-$RC_6H_4N(CH_2S)_2$ (R = H, Cl, MeO) that is bridged between the two Ni atoms in CpNi and (dppv) Ni or (dppe)Ni moieties. In addition, on the basis of electrochemical and electrocatalytic studies, we have found that targeted complexes **8** and **9** can serve as the catalysts for proton reduction to H_2 using HOAc as the proton source under CV conditions. Finally, it should be indicated that (i) the azadithiolato-bridged dinuclear complexes **8** and **9** are better catalysts than the dithiolato-bridged dinuclear complexes $Cp_2Ni_2(\mu$-$SR)_2$ (R = $PhCH_2$, C_8H_{17}, C_6H_4Me) for the H_2 production from HOAc under the electrochemical conditions, since the former have much higher i_{cat}/i_p values and much lower overpotentials in comparison to those of the latter, and (ii) in view of the structural similarity of our targeted dinuclear complexes **8**−**11** with the active site of [NiFe]-H_2ases as well as the catalytic functional similarity of the representative targeted complexes **8** and **9** with [NiFe]-H_2ases, the targeted complexes reported in this article could be regarded as biomimetic mimics for [NiFe]-H_2ases.

■ EXPERIMENTAL SECTION

General Comments. All reactions were performed using standard Schlenk and vacuum-line techniques under an atmosphere of argon. Tetrahydrofuran (THF) was distilled under Ar from sodium/benzophenone ketyl, whereas methylene chloride was distilled under Ar from CaH_2. Ethanol, $MeNO_2$, t-BuONa, 4-$RC_6H_4NH_2$ (R = H, Cl, MeO), thioacetic acid, and 37% aqueous formaldehyde were available commercially, whereas $[(C_5H_5)_3Ni_2]BF_4$,[49] (dppv)$NiCl_2$ (dppv = 1,2-bis(diphenylphosphino)ethane),[68] and (dppe)$NiCl_2$ (dppe = 1,2-bis(diphenylphosphino)ethane)[68] were prepared according to the published procedures. While ^1H, $^{13}C\{^1H\}$, and $^{31}P\{^1H\}$ NMR spectra were obtained on a Bruker Avance 400 NMR spectrometer, IR spectra were recorded on a Bio-Rad FTS 135 infrared spectrophotometer. Elemental analyses were performed on an Elementar Vario EL analyzer. Melting points were determined on a SGW X-4 microscopic melting point apparatus and were uncorrected.

Preparation of $C_6H_5N[CH_2S(O)CMe]_2$ (1). A 250 mL three-necked flask was charged with aniline (9.1 mL, 100 mmol), 37% aqueous formaldehyde (24.2 mL, 320 mmol), thioacetic acid (14.6 mL, 200 mmol), and ethanol (100 mL). While it was stirred, the mixture was heated to about 60 °C and stirred at this temperature for 3 h. To the resulting mixture was added 100 mL of ice−water to give precipitates. The precipitates were collected by filtration, washed with some cold ethanol, and finally dried under vacuum to give **1** (21.7 g, 81%) as a white solid, mp 66−67 °C. Anal. Calcd for $C_{12}H_{15}NO_2S_2$: C, 53.51; H, 5.61; N, 5.20. Found: C, 53.55; H, 5.76; N, 5.23. IR (KBr disk): $\nu_{C=O}$ 1690 (vs) cm^{-1}. ^1H NMR (400 MHz, $CDCl_3$): 2.38 (s, 6H, $2CH_3$), 5.12 (s, 4H, CH_2NCH_2), 6.77−7.31 (m, 5H, C_6H_5) ppm. $^{13}C\{^1H\}$ NMR (100 MHz, $CDCl_3$): 31.4 (s, CH_3), 52.9 (s, CH_2NCH_2), 114.6−144.0 (m, C_6H_5), 196.0 (s, C=O) ppm.

https://dx.doi.org/10.1021/acs.organomet.0c00130
Organometallics XXXX, XXX, XXX−XXX

Preparation of (4-ClC$_6$H$_4$)N[CH$_2$S(O)CMe]$_2$ (2). The same procedure was followed as for **1**, except that 4-chloroaniline (12.8 g, 100 mmol) was used instead of aniline. **2** (23.7 g, 78%) was obtained as a white solid, mp 82−83 °C. Anal. Calcd for $C_{12}H_{14}ClNO_2S_2$: C, 47.44; H, 4.64; N, 4.61. Found: C, 47.33; H, 4.74; N, 4.52. IR (KBr disk): $\nu_{C=O}$ 1690 (vs) cm^{-1}. ^{1}H NMR (400 MHz, CDCl$_3$): 2.37 (s, 6H, 2CH$_3$), 5.06 (s, 4H, CH$_2$NCH$_2$), 6.68−7.23 (m, 4H, C$_6$H$_4$) ppm. ^{13}C{^{1}H} NMR (100 MHz, CDCl$_3$): 31.3 (s, CH$_3$), 52.8 (s, CH$_2$NCH$_2$), 115.8−142.5 (m, C$_6$H$_4$), 195.8 (s, C═O) ppm.

Preparation of (4-MeOC$_6$H$_4$)N[CH$_2$S(O)CMe]$_2$ (3). The same procedure was followed as for **1**, except that 4-methoxyaniline (12.3 g, 100 mmol) was utilized instead of aniline. **3** (22.4 g, 75%) was obtained as a white solid, mp 73−74 °C. Anal. Calcd for $C_{13}H_{17}NO_3S_2$: C, 52.15; H, 5.72; N, 4.68. Found: C, 52.26; H, 5.90; N, 4.61. IR (KBr disk): $\nu_{C=O}$ 1687 (vs) cm^{-1}. ^{1}H NMR (400 MHz, CDCl$_3$): 2.36 (s, 6H, 2CH$_3$C═O), 3.76 (s, 3H, OCH$_3$), 5.07 (s, 4H, CH$_2$NCH$_2$), 6.74−6.86 (m, 4H, C$_6$H$_4$) ppm. ^{13}C{^{1}H} NMR (100 MHz, CDCl$_3$): 31.4 (s, CH$_3$C═O), 53.7 (s, CH$_2$NCH$_2$), 55.7 (s, OCH$_3$), 114.9−154.1 (m, C$_6$H$_4$), 196.1 (s, C═O) ppm.

Preparation of (dppv)Ni[(SCH$_2$)$_2$NC$_6$H$_5$] (4). A 100 mL three-necked flask was charged with C$_6$H$_5$N[CH$_2$S(O)CMe]$_2$ (0.269 g, 1.0 mmol), *t*-BuONa (0.192 g, 2.0 mmol), and THF (40 mL). The mixture was stirred at −78 °C for 3 h to give a pale yellow solution. To this solution was slowly added (dppv)NiCl$_2$(0.526 g, 1.0 mmol) in 10 mL of THF to give a brown-red solution. After the brown-red solution was stirred at −78 °C for 4 h, it was warmed to room temperature and stirred at this temperature for 1 h. The solvent was removed at reduced pressure, and the residue was subjected to column chromatography (silica gel). Elution with CH$_2$Cl$_2$/acetone (25/1 v/v) developed a red band, from which **4** (0.313 g, 49%) was obtained as a red solid, mp 197−198 °C. Anal. Calcd for $C_{34}H_{31}NNiP_2S_2$: C, 63.97; H, 4.89; N, 2.19. Found: C, 63.77; H, 4.91; N, 2.15. IR (KBr disk): 1496 (m), 1434 (m), 1265 (s), 1099 (s), 1037 (s) cm^{-1}. ^{1}H NMR (400 MHz, CDCl$_3$): 4.44 (s, 4H, CH$_2$NCH$_2$), 6.77−7.52 (m, 27H, 5C$_6$H$_5$, CH═CH) ppm. ^{13}C{^{1}H} NMR (100 MHz, CDCl$_3$): 48.0 (s, CH$_2$NCH$_2$), 117.6−149.2 (m, C$_6$H$_5$, CH═CH) ppm. ^{31}P{^{1}H} NMR (162 MHz, CDCl$_3$): 63.3 (s, NiP$_2$) ppm.

Preparation of (dppv)Ni[(SCH$_2$)$_2$NC$_6$H$_4$Cl-4] (5). The same procedure as for **4** was followed, except that C$_6$H$_5$N[CH$_2$S(O)CMe]$_2$ was replaced by (4-ClC$_6$H$_4$)N[CH$_2$S(O)CMe]$_2$ (0.304 g, 1.0 mmol). **5** (0.276 g, 41%) was obtained as a red solid, mp 158−159 °C. Anal. Calcd for $C_{34}H_{30}ClNNiP_2S_2$: C, 60.69; H, 4.49; N, 2.08. Found: C, 60.39; H, 4.65; N, 1.78. IR (KBr disk): 1494 (m), 1434 (m), 1267 (s), 1053 (vs) cm^{-1}. ^{1}H NMR (400 MHz, CDCl$_3$): 4.47 (s, 4H, CH$_2$NCH$_2$), 6.83−7.62 (m, 26H, 4C$_6$H$_5$, C$_6$H$_4$, CH═CH) ppm. ^{13}C{^{1}H} NMR (100 MHz, CDCl$_3$): 48.2 (s, CH$_2$NCH$_2$), 119.3−147.1 (m, C$_6$H$_5$, C$_6$H$_4$, CH═CH) ppm. ^{31}P{^{1}H} NMR (162 MHz, CDCl$_3$): 63.3 (s, NiP$_2$) ppm.

Preparation of (dppe)Ni[(SCH$_2$)$_2$NC$_6$H$_5$] (6). The same procedure as for **4** was followed, except that (dppv)NiCl$_2$ was replaced by (dppe)NiCl$_2$ (0.528 g, 1.0 mmol). **6** (0.290 g, 45%) was obtained as a red solid, mp 120 °C dec. Anal. Calcd for $C_{34}H_{33}NNiP_2S_2$: C, 63.77; H, 5.19; N, 2.19. Found: C, 63.88; H, 5.29; N, 2.25. IR (KBr disk): 1594 (m), 1496 (m), 1435 (s), 1098 (vs), 1059 (vs) cm^{-1}. ^{1}H NMR (400 MHz, CDCl$_3$): 2.05, 2.09 (2s, 4H, CH$_2$CH$_2$), 4.50 (s, 4H, CH$_2$NCH$_2$), 6.87−7.68 (m, 25H, 5C$_6$H$_5$) ppm. ^{13}C{^{1}H} NMR (100 MHz, CDCl$_3$): 27.7−28.2 (m, CH$_2$CH$_2$), 47.4 (s, CH$_2$NCH$_2$), 117.4−145.9 (m, C$_6$H$_5$) ppm. ^{31}P{^{1}H} NMR (162 MHz, CDCl$_3$): 56.6 (s, NiP$_2$) ppm.

Preparation of (dppe)Ni[(SCH$_2$)$_2$NC$_6$H$_4$OMe-4] (7). The same procedure was followed as for **6**, except that C$_6$H$_5$N[CH$_2$S(O)CMe]$_2$ was replaced by (4-MeOC$_6$H$_4$)N[CH$_2$S(O)CMe]$_2$ (0.299 g, 1.0 mmol). **7** (0.288 g, 43%) was obtained as a red solid, mp 143−144 °C. Anal. Calcd for $C_{35}H_{35}NNiOP_2S_2$: C, 62.70; H, 5.26; N, 2.09. Found: C, 62.53; H, 5.32; N, 2.08. IR (KBr disk): 1510 (vs), 1435 (s), 1273 (s), 1101 (vs), 1041 (vs) cm^{-1}. ^{1}H NMR (400 MHz, CDCl$_3$): 2.05, 2.09 (2s, 4H, CH$_2$CH$_2$), 3.88 (s, 3H, OCH$_3$), 4.47 (s, 4H, CH$_2$NCH$_2$), 6.85−7.70 (m, 24H, 4C$_6$H$_5$, C$_6$H$_4$) ppm. ^{13}C{^{1}H} NMR (100 MHz, CDCl$_3$): 27.8−28.3 (m, CH$_2$CH$_2$), 48.3 (s, CH$_2$NCH$_2$), 55.9 (s, OCH$_3$), 114.1−151.9 (m, C$_6$H$_5$, C$_6$H$_4$) ppm. ^{31}P{^{1}H} NMR (162 MHz, CDCl$_3$): 57.3 (s, NiP$_2$) ppm.

Preparation of [(η^5-C$_5$H$_5$)Ni{(μ-SCH$_2$)$_2$NC$_6$H$_5$}Ni(dppv)]BF$_4$ (8). A 50 mL three-necked flask was charged with (dppv)Ni-[(SCH$_2$)$_2$NC$_6$H$_5$] (0.128 g, 0.2 mmol), [(C$_5$H$_5$)$_3$Ni$_2$]BF$_4$ (0.080 g, 0.2 mmol), and MeNO$_2$ (10 mL). The mixture was stirred at room temperature for 0.5 h to give a brown-red solution. The solvent was removed at reduced pressure to leave a residue, which was subjected to column chromatography (silica gel). Elution with CH$_2$Cl$_2$/acetone (10/1 v/v) developed a brown band, from which **8** (0.117 g, 69%) was obtained as a brown solid, mp 92−93 °C. Anal. Calcd for $C_{39}H_{36}BF_4NNi_2P_2S_2$: C, 55.18; H, 4.27; N, 1.65. Found: C, 54.98; H, 4.32; N, 1.40. IR (KBr disk): 1495 (s), 1438 (s), 1268 (s), 1059 (vs), 738 (vs) cm^{-1}. ^{1}H NMR (400 MHz, CDCl$_3$): 4.26, 4.52 (dd, *J* = 11.4 Hz, 4H, CH$_2$NCH$_2$), 4.81 (s, 5H, C$_5$H$_5$), 6.50−7.81 (m, 27H, 5C$_6$H$_5$, CH═CH) ppm. ^{13}C{^{1}H} NMR (100 MHz, CDCl$_3$): 55.1 (s, CH$_2$NCH$_2$), 91.8 (s, C$_5$H$_5$), 118.0−146.5 (m, C$_6$H$_5$, CH═CH) ppm. ^{31}P{^{1}H} NMR (162 MHz, CDCl$_3$): 70.0 (s, NiP$_2$) ppm.

Preparation of [(η^5-C$_5$H$_5$)Ni{(μ-SCH$_2$)$_2$NC$_6$H$_4$Cl-4}Ni(dppv)]-(BF$_4$) (9). The same procedure was followed as for **8**, except that (dppv)Ni[(SCH$_2$)$_2$NC$_6$H$_5$] was replaced by (dppv)Ni-[(SCH$_2$)$_2$NC$_6$H$_4$Cl-4] (0.135 g, 0.2 mmol). **9** (0.159 g, 90%) was obtained as a brown solid, mp 247 °C dec. Anal. Calcd for $C_{39}H_{35}BClF_4NNi_2P_2S_2$: C, 53.02; H, 3.99; N, 1.59. Found: C, 53.29; H, 3.73; N, 1.50. IR (KBr disk):1492 (s), 1437 (s), 1267 (s), 1057 (vs), 738 (vs) cm^{-1}. ^{1}H NMR (400 MHz, CDCl$_3$): 4.20, 4.51 (dd, *J* = 12.2 Hz, 4H, CH$_2$NCH$_2$), 4.91 (s, 5H, C$_5$H$_5$), 6.32−7.87 (m, 26H, 4C$_6$H$_5$, C$_6$H$_4$, CH═CH) ppm. ^{13}C{^{1}H} NMR (100 MHz, CDCl$_3$): 54.9 (s, CH$_2$NCH$_2$), 92.1 (s, C$_5$H$_5$), 119.2−147.1 (m, C$_6$H$_5$, C$_6$H$_4$, CH═CH) ppm. ^{31}P{^{1}H} NMR (162 MHz, CDCl$_3$): 70.2 (s, NiP$_2$) ppm.

Preparation of [(η^5-C$_5$H$_5$)Ni{(μ-SCH$_2$)$_2$NC$_6$H$_5$}Ni(dppe)]BF$_4$ (10). The same procedure was followed as for **8**, except that (dppv)Ni[(SCH$_2$)$_2$NC$_6$H$_5$] was replaced by (dppe)Ni-[(SCH$_2$)$_2$NC$_6$H$_5$] (0.128 g, 0.2 mmol). **10** (0.157 g, 92%) was obtained as a brown solid, mp 117−118 °C. Anal. Calcd for $C_{39}H_{38}BF_4NNi_2P_2S_2$: C, 55.04; H, 4.50; N, 1.65. Found: C, 55.30; H, 4.37; N, 1.43. IR (KBr disk): 1642 (m), 1431 (m), 1267 (s), 1057 (vs), 740 (vs) cm^{-1}. ^{1}H NMR (400 MHz, CDCl$_3$): 2.54−2.64 (m, 4H, CH$_2$CH$_2$), 4.21, 4.46 (dd, *J* = 12.0 Hz, 4H, CH$_2$NCH$_2$), 5.05 (s, 5H, C$_5$H$_5$), 6.48−7.95 (m, 25H, 5C$_6$H$_5$) ppm. ^{13}C{^{1}H} NMR (100 MHz, CDCl$_3$): 27.1−27.6 (m, CH$_2$CH$_2$), 55.1 (s, CH$_2$NCH$_2$), 92.1 (s, C$_5$H$_5$), 118.1−143.9 (m, C$_6$H$_5$) ppm. ^{31}P{^{1}H} NMR (162 MHz, CDCl$_3$): 61.4 (s, NiP$_2$) ppm.

Preparation of [(η^5-C$_5$H$_5$)Ni{(μ-SCH$_2$)$_2$NC$_6$H$_4$OMe-4}Ni-(dppe)]BF$_4$ (11). The same procedure was followed as for **10**, except that (dppe)Ni[(SCH$_2$)$_2$NC$_6$H$_5$] was replaced by (dppe)Ni-[(SCH$_2$)$_2$NC$_6$H$_4$OMe-4] (0.134 g, 0.2 mmol). **11** (0.143 g, 81%) was obtained as a brown solid, mp 104−105 °C. Anal. Calcd for $C_{40}H_{40}BF_4NNi_2OP_2S_2$: C, 54.53; H, 4.58; N, 1.59. Found: C, 54.29; H, 4.71; N, 1.42. IR (KBr disk): 1643 (m), 1430 (m), 1266 (s), 1057 (vs), 740 (vs) cm^{-1}. ^{1}H NMR (400 MHz, CDCl$_3$): 2.51−2.54 (m, 4H, CH$_2$CH$_2$), 3.77 (s, 3H, OCH$_3$), 4.12, 4.50 (dd, *J* = 11.8 Hz, 4H, CH$_2$NCH$_2$), 5.12 (s, 5H, C$_5$H$_5$), 6.38−8.00 (m, 24H, 4C$_6$H$_5$, C$_6$H$_4$) ppm. ^{13}C{^{1}H} NMR (100 MHz, CDCl$_3$): 27.0−27.5 (m, CH$_2$CH$_2$), 55.7 (s, CH$_2$NCH$_2$), 56.5 (s, OCH$_3$), 92.0 (s, C$_5$H$_5$), 114.9−154.7 (m, C$_6$H$_5$, C$_6$H$_4$) ppm. ^{31}P{^{1}H} NMR (162 MHz, CDCl$_3$): 60.8 (s, NiP$_2$) ppm.

X-ray Crystal Structure Determinations of 5, 9, and 11. White single crystals of **5**, **9**, and **11** for X-ray diffraction analysis were grown by slow diffusion of hexane into their CH$_2$Cl$_2$ solutions at −5 °C. A single crystal of **5**, **9**, or **11** was mounted on a Rigaku MM-007 (rotating anode) diffractometer equipped with an AtlasS2 accessory. While the data for **5** and **11** were collected using a confocal monochromator with Cu Kα radiation (λ = 1.54184 Å) in the ω scanning mode at 156 and 137 K, respectively, data for **9** were collected using a confocal monochromator with Mo Kα radiation (λ = 0.71073 Å) in the ω scanning mode at 293 K. Data collection, reduction, and absorption correction were performed by the

https://dx.doi.org/10.1021/acs.organomet.0c00130
Organometallics XXXX, XXX, XXX−XXX

Table 4. Crystal Data and Structure Refinement Details for 5, 9, and 11

	5	9	11
mol formula	$C_{34}H_{30}ClNNiP_2S_2$	$C_{39}H_{35}BClF_4NNi_2P_2S_2$	$C_{40}H_{40}BF_4NNi_2OP_2S_2 \cdot CH_2Cl_2$
mol wt	672.81	883.42	965.94
cryst syst	monoclinic	orthorhombic	monoclinic
space group	$P1_21/c1$	$P2_12_12_1$	$P1_21/n1$
a/Å	9.7904(3)	10.8883(6)	13.7926(6)
b/Å	22.7021(6)	14.1424(6)	20.2017(8)
c/Å	14.9176(3)	24.6398(12)	14.8223(6)
α/deg	90	90	90
β/deg	100.961(3)	90	91.602(3)
γ/deg	90	90	90
V/Å^3	3255.14(15)	3794.2(3)	4128.4(3)
Z	4	4	4
D_c/g cm^{-3}	1.373	1.547	1.554
abs coeff/mm^{-1}	3.926	1.308	4.450
F(000)	1392	1808	1984
index ranges	$-11 \le h \le 11$	$-12 \le h \le 12$	$-16 \le h \le 12$
	$-24 \le k \le 27$	$-16 \le k \le 14$	$-17 \le k \le 23$
	$-17 \le l \le 12$	$-29 \le l \le 25$	$-13 \le l \le 17$
no. of rflns	12434	16389	14646
no. of indep rflns	5812	6670	6788
$2\theta_{max}$/deg	134.15	50.02	127.37
R	0.0522	0.0406	0.0699
R_w	0.1426	0.0731	0.1884
GOF	1.031	1.010	1.042
largest diff peak, hole/e Å^{-3}	0.847/−0.578	0.451/−0.490	1.996 /−0.646

CRYSTALCLEAR program.[69] The structures were solved by direct methods using the SHELXS program[70] and refined by full-matrix least-squares techniques (SHELXL)[71] on F^2. Hydrogen atoms were located by using the geometric method. Details of crystal data, data collections, and structure refinements are summarized in Table 4.

■ ASSOCIATED CONTENT

Supporting Information

The Supporting Information is available free of charge at https://pubs.acs.org/doi/10.1021/acs.organomet.0c00130.

Electrochemical and electrocatalytic data, overpotential determinations, and IR and NMR spectra of compounds **3**, **4**, **6**, and **8−11** (PDF)

Accession Codes

CCDC 1984978−1984980 contain the supplementary crystallographic data for this paper. These data can be obtained free of charge via www.ccdc.cam.ac.uk/data_request/cif, or by emailing data_request@ccdc.cam.ac.uk, or by contacting The Cambridge Crystallographic Data Centre, 12 Union Road, Cambridge CB2 1EZ, UK; fax: +44 1223 336033.

■ AUTHOR INFORMATION

Corresponding Author

Li-Cheng Song − *Department of Chemistry, State Key Laboratory of Elemento-Organic Chemistry, College of Chemistry, Nankai University, Tianjin 300071, People's Republic of China; Collaborative Innovation Center of Chemical Science and Engineering (Tianjin), Tianjin 300072, People's Republic of China;* orcid.org/0000-0003-0964-8869; Email: lcsong@nankai.edu.cn

Authors

Wen-Bo Liu − *Department of Chemistry, State Key Laboratory of Elemento-Organic Chemistry, College of Chemistry, Nankai University, Tianjin 300071, People's Republic of China*

Bei-Bei Liu − *Department of Chemistry, State Key Laboratory of Elemento-Organic Chemistry, College of Chemistry, Nankai University, Tianjin 300071, People's Republic of China*

Complete contact information is available at: https://pubs.acs.org/10.1021/acs.organomet.0c00130

Notes

The authors declare no competing financial interest.

■ ACKNOWLEDGMENTS

We are grateful to the National Natural Science Foundation of China (21772106) and Technology of China (973 program 2014CB845604) for financial support.

■ REFERENCES

(1) Adams, M. W. W.; Stiefel, E. I. Biological Hydrogen Production: Not So Elementary. *Science* **1998**, *282*, 1842−1843.
(2) Cammack, R. Hydrogenase sophistication. *Nature* **1999**, *397*, 214−215.
(3) Albracht, S. P. J. Nickel hydrogenases: in search of the active site. *Biochim. Biophys. Acta, Bioenerg.* **1994**, *1188*, 167−204.
(4) Fontecilla-Camps, J. C.; Volbeda, A.; Cavazza, C.; Nicolet, Y. Structure/Function Relationships of [NiFe]- and [FeFe]-Hydrogenases. *Chem. Rev.* **2007**, *107*, 4273−4303.
(5) Bouwman, E.; Reedijk, J. Structural and functional models related to the nickel hydrogenases. *Coord. Chem. Rev.* **2005**, *249*, 1555−1581.
(6) Nicolet, Y.; Lemon, B. J.; Fontecilla-Camps, J. C.; Peters, J. W. A novel FeS cluster in Fe-only hydrogenases. *Trends Biochem. Sci.* **2000**, *25*, 138−143.

(7) Evans, D. J.; Pickett, C. J. Chemistry and the hydrogenases. *Chem. Soc. Rev.* **2003**, *32*, 268−275.
(8) Frey, M. Hydrogenases: Hydrogen-Activating Enzymes. *ChemBioChem* **2002**, *3*, 153−160.
(9) Shima, S.; Pilak, O.; Vogt, S.; Schick, M.; Stagni, M. S.; Meyer-Klaucke, W.; Warkentin, E.; Thauer, R. K.; Ermler, U. The Crystal Structure of [Fe]-Hydrogenase Reveals the Geometry of the Active Site. *Science* **2008**, *321*, 572−575.
(10) Shima, S.; Thauer, R. K. A Third Type of Hydrogenase Catalyzing H_2 Activation. *Chem. Rec.* **2007**, *7*, 37−46.
(11) Wright, J. A.; Turrell, P. J.; Pickett, C. J. The Third Hydrogenase: More Natural Organometallics. *Organometallics* **2010**, *29*, 6146−6156.
(12) Volbeda, A.; Charon, M.-H.; Piras, C.; Hatchikian, E. C.; Frey, M.; Fontecilla-Camps, J. C. Crystal structure of the nickel-iron hydrogenase from *Desulfovibrio gigas*. *Nature* **1995**, *373*, 580−587.
(13) Volbeda, A.; Garcin, E.; Piras, C.; de Lacey, A. L.; Fernandez, V. M.; Hatchikian, E. C.; Frey, M.; Fontecilla-Camps, J. C. Structure of the [NiFe] Hydrogenase Active Site: Evidence for Biologically Uncommon Fe Ligands. *J. Am. Chem. Soc.* **1996**, *118*, 12989−12996.
(14) Higuchi, Y.; Ogata, H.; Miki, K.; Yasuoka, N.; Yagi, T. Removal of the bridging ligand atom at the Ni-Fe active site of [NiFe] hydrogenase upon reduction with H_2, as revealed by X-ray structure analysis at 1.4 Å resolution. *Structure* **1999**, *7*, 549−556.
(15) Lubitz, W.; Ogata, H.; Rüdiger, O.; Reijerse, E. Hydrogenases. *Chem. Rev.* **2014**, *114*, 4081−4148.
(16) Schilter, D.; Camara, J. M.; Huynh, M. T.; Hammes-Schiffer, S.; Rauchfuss, T. B. Hydrogenase Enzymes and Their Synthetic Models: The Role of Metal Hydrides. *Chem. Rev.* **2016**, *116*, 8693−8749.
(17) Simmons, T. R.; Berggren, G.; Bacchi, M.; Fontecave, M.; Artero, V. Mimicking hydrogenases: From biomimetics to artificial enzymes. *Coord. Chem. Rev.* **2014**, *270−271*, 127−150.
(18) Ogo, S. H_2 and O_2 activation by [NiFe]hydrogenases-Insights from model complexes. *Coord. Chem. Rev.* **2017**, *334*, 43−53.
(19) Zhu, W.; Marr, A. C.; Wang, Q.; Neese, F.; Spencer, D. J. E.; Blake, A. J.; Cooke, P. A.; Wilson, C.; Schröder, M. Modulation of the electronic structure and the Ni-Fe distance in heterobimetallic models for the active site in [NiFe]hydrogenase. *Proc. Natl. Acad. Sci. U. S. A.* **2005**, *102*, 18280−18285.
(20) Wang, Q.; Barclay, J. E.; Blake, A. J.; Davies, E. S.; Evans, D. J.; Marr, A. C.; McInnes, E. J. L.; McMaster, J.; Wilson, C.; Schröder, M. The Synthesis and Electronic Structure of a Novel $[NiS_4Fe_2(CO)_6]$ Radical Cluster: Implications for the Active Site of the [NiFe] Hydrogenases. *Chem. - Eur. J.* **2004**, *10*, 3384−3396.
(21) Osterloh, F.; Saak, W.; Haase, D.; Pohl, S. Synthesis, X-ray structure and electrochemical characterisation of a binuclear thiolate bridged Ni-Fe-nitrosyl complex, related to the active site of NiFe hydrogenase. *Chem. Commun.* **1997**, 979−980.
(22) Yang, X.; Elrod, L. C.; Reibenspies, J. H.; Hall, M. B.; Darensbourg, M. Y. Oxygen uptake in complexes related to [NiFeS]- and [NiFeSe]-hydrgenase active sites. *Chem. Sci.* **2019**, *10*, 1368−1373.
(23) Carroll, M. E.; Barton, B. E.; Gray, D. L.; Mack, A. E.; Rauchfuss, T. B. Active-Site Models for the Nickel-Iron Hydrogenases: Effects of Ligands on Reactivity and Catalytic Properties. *Inorg. Chem.* **2011**, *50*, 9554−9563.
(24) Smith, M. C.; Barclay, J. E.; Cramer, S. P.; Davies, S. C.; Gu, W.-W.; Hughes, D. L.; Longhurst, S.; Evans, D. J. Nickel-iron-sulfur complexes: approaching structural analogues of the active sites of NiFe-hydrogenase and carbon monoxide dehydrogenase/acetyl-CoA synthase. *J. Chem. Soc., Dalton Trans.* **2002**, 2641−2647.
(25) Verhagen, J. A. W.; Lutz, M.; Spek, A. L.; Bouwman, E. Synthesis and Characterisation of New Nickel-Iron Complexes with an S_4 Coordination Environment around the Nickel Centre. *Eur. J. Inorg. Chem.* **2003**, *2003*, 3968−3974.
(26) Li, Z.; Ohki, Y.; Tatsumi, K. Dithiolato-Bridged Dinuclear Iron-Nickel Complexes $[Fe(CO)_2(CN)_2(\mu\text{-}SCH_2CH_2CH_2S)Ni(S_2CNR_2)]^-$ Modeling the Active Site of [NiFe] Hydrogenase. *J. Am. Chem. Soc.* **2005**, *127*, 8950−8951.
(27) Sellmann, D.; Lauderbach, F.; Heinemann, F. W. Trinuclear [NiFe] Clusters as Structural Models for [NiFe] Hydrogenase Active Sites. *Eur. J. Inorg. Chem.* **2005**, *2005*, 371−377.
(28) Ogo, S.; Ichikawa, K.; Kishima, T.; Matsumoto, T.; Nakai, H.; Kusaka, K.; Ohhara, T. A Functional [NiFe]Hydrogenase Mimic That Catalyzes Electron and Hydride Transfer from H_2. *Science* **2013**, *339*, 682−684.
(29) Ohki, Y.; Yasumura, K.; Ando, M.; Shimokata, S.; Tatsumi, K. A model for the CO-inhibited form of [NiFe] hydrogenase: synthesis of $(CO)_3Fe(\mu\text{-}S^tBu)_3Ni\{SC_6H_3\text{-}2,6\text{-}(mesityl)_2\}$ and reversible CO addition at the Ni site. *Proc. Natl. Acad. Sci. U. S. A.* **2010**, *107*, 3994−3997.
(30) Ogo, S.; Kabe, R.; Uehara, K.; Kure, B.; Nishimura, T.; Menon, S. C.; Harada, R.; Fukuzumi, S.; Higuchi, Y.; Ohhara, T.; Tamada, T.; Kuroki, R. A Dinuclear Ni(μ-H)Ru Complex Derived from H_2. *Science* **2007**, *316*, 585−587.
(31) Brazzolotto, D.; Gennari, M.; Queyriaux, N.; Simmons, T. R.; Pécaut, J.; Demeshko, S.; Meyer, F.; Orio, M.; Artero, V.; Duboc, C. Nickel-centred proton reduction catalysis in a model of [NiFe] hydrogenase. *Nat. Chem.* **2016**, *8*, 1054−1060.
(32) Song, L.-C.; Yang, X.-Y.; Cao, M.; Gao, X.-Y.; Liu, B.-B.; Zhu, L.; Jiang, F. Dithiolato-bridged nickel-iron complexes as models for the active site of [NiFe]-hydrogenases. *Chem. Commun.* **2017**, *53*, 3818−3821.
(33) Song, L.-C.; Yang, X.-Y.; Gao, X.-Y.; Cao, M. Nickel-Iron Dithiolato Hydrides Derived from H_2 Activation by Their μ-Hydroxo Ligand-Containing Analogues. *Inorg. Chem.* **2019**, *58*, 39−42.
(34) Lindenmaier, N. J.; Wahlefeld, S.; Bill, E.; Szilvási, T.; Eberle, C.; Yao, S.; Hildebrandt, P.; Horch, M.; Zebger, I.; Driess, M. An S-Oxygenated [NiFe] Complex Modelling Sulfenate Intermediates of an O_2-Tolerant Hydrogenase. *Angew. Chem., Int. Ed.* **2017**, *56*, 2208−2211.
(35) Chambers, G. M.; Rauchfuss, T. B.; Arrigoni, F.; Zampella, G. Effect of Pyramidalization of the $M_2(SR)_2$ Center: The Case of $(C_5H_5)_2Ni_2(SR)_2$. *Organometallics* **2016**, *35*, 836−846.
(36) Schilter, D.; Fuller, A. L.; Gray, D. L. Nickel-Molybdenum and Nickel-Tungsten Dithiolates: Hybrid Models for Hydrogenases and Hydrodesulfurization. *Eur. J. Inorg. Chem.* **2015**, *2015*, 4638−4642.
(37) Rosenkoetter, K. E.; Ziller, J. W.; Heyduk, A. F. A Heterobimetallic W-Ni Complex Containing a Redox-Active W-$[SNS]_2$ Metalloligand. *Inorg. Chem.* **2016**, *55*, 6794−6798.
(38) Song, L.-C.; Zhang, L.-D.; Zhang, W.-W.; Liu, B.-B. Heterodinuclear Ni/M (M = Mo, W) Complexes Relevant to the Active Site of [NiFe]-Hydrogenases: Synthesis, Characterization, and Electrocatalytic H_2 Evolution. *Organometallics* **2018**, *37*, 1948−1957.
(39) Ogo, S.; Mori, Y.; Ando, T.; Matsumoto, T.; Yatabe, T.; Yoon, K.-S.; Hayashi, H.; Asano, M. One Model, Two Enzymes: Activation of Hydrogen and Carbon Monoxide. *Angew. Chem., Int. Ed.* **2017**, *56*, 9723−9726.
(40) Kure, B.; Sano, M.; Watanabe, N.; Nakajima, T.; Tanase, T. Synthesis and Reactivity of Thiolate-Bridged $Ni^{II}M^{I}$ Heterodinuclear Complexes (M = Rh, Ir) with an S-Bidentate NiP_2S_2 Metalloligand. *Eur. J. Inorg. Chem.* **2017**, *2017*, 4097−4109.
(41) Fourmond, V.; Canaguier, S.; Golly, B.; Field, M. J.; Fontecave, M.; Artero, V. A nickel-manganese catalyst as a biomimic of the active site of NiFe hydrogenases: a combined electrocatalytical and DFT mechanistic study. *Energy Environ. Sci.* **2011**, *4*, 2417−2427.
(42) Song, L.-C.; Li, J.-P.; Xie, Z.-J.; Song, H.-B. Synthesis, Structural Characterization, and Electrochemical Properties of Dinuclear Ni/Mn Model Complexes for the Active Site of [NiFe]-Hydrogenases. *Inorg. Chem.* **2013**, *52*, 11618−11626.
(43) Chu, X.; Jin, J.; Ming, B.; Pang, M.; Yu, X.; Tung, C.-H.; Wang, W. Bimetallic nickel-cobalt hydrides in H_2 activation and catalytic proton reduction. *Chem. Sci.* **2019**, *10*, 761−767.
(44) Fan, H.-J.; Hall, M. B. A Capable Bridging Ligand for Fe-Only Hydrogenase: Density Functional Calculations of a Low-Energy Route for Heterolytic Cleavage and Formation of Dihydrogen. *J. Am. Chem. Soc.* **2001**, *123*, 3828−3829.

(45) Silakov, A.; Wenk, B.; Reijerse, E.; Lubitz, W. ^{14}N HYSCORE investigation of the H-cluster of [FeFe] hydrogenase: evidence for a nitrogen in the dithiol bridge. *Phys. Chem. Chem. Phys.* **2009**, *11*, 6592−6599.
(46) Berggren, G.; Adamska, A.; Lambertz, C.; Simmons, T. R.; Esselborn, J.; Atta, M.; Gambarelli, S.; Mouesca, J.-M.; Reijerse, E.; Lubitz, W.; Happe, T.; Artero, V.; Fontecave, M. Biomimetic assembly and activation of [FeFe]-hydrogenases. *Nature* **2013**, *499*, 66−69.
(47) Izawa, T.; Terao, Y.; Suzuki, K. Syntheses of optically active γ-ketothiols and the esters by lipase-catalyzed hydrolysis via α-acetylthiomethylation of ketones. *Tetrahedron: Asymmetry* **1997**, *8*, 2645−2648.
(48) Angamuthu, R.; Chen, C.-S.; Cochrane, T. R.; Gray, D. L.; Schilter, D.; Ulloa, O. A.; Rauchfuss, T. B. N-Substituted Derivatives of the Azadithiolate Cofactor from the [FeFe] Hydrogenases: Stability and Complexation. *Inorg. Chem.* **2015**, *54*, 5717−5724.
(49) Salzer, A.; Werner, H. A New Route to Triple-Decker Sandwich Compounds. *Angew. Chem., Int. Ed. Engl.* **1972**, *11*, 930−932.
(50) Cordero, B.; Gómerz, V.; Platero-Prats, A. E.; Revés, M.; Echeverría, J.; Cremades, E.; Barragán, F.; Alvarez, S. Covalent radii revisited. *Dalton Trans.* **2008**, 2832−2838.
(51) Redin, K.; Wilson, A. D.; Newell, R.; DuBois, M. R.; DuBois, D. L. Studies of Structural Effects on the Half-Wave Potentials of Mononuclear and Dinuclear Nickel(II) Diphosphine/Dithiolate Complexes. *Inorg. Chem.* **2007**, *46*, 1268−1276.
(52) Goh, Y. X. C.; Tang, H. M.; Loke, W. L. J.; Fan, W. Y. Bis(cyclopentadienyl)nickel(II) μ-Thiolato Complexes as Proton Reduction Electrocatalysts. *Inorg. Chem.* **2019**, *58*, 12178−12183.
(53) Bhandari, A.; Maji, R. C.; Mishra, S.; Kumar, A.; Barman, S. K.; Das, P. P.; Ghiassi, K. B.; Olmstead, M. M.; Patra, A. K. Model Complexes for the Ni_p Site of Acetyl Coenzyme A Synthase/Carbon Monoxide (CO) Dehydrogenase: Structure, Electrochemistry, and CO Reactivity. *Inorg. Chem.* **2018**, *57*, 13713−13727.
(54) Luo, S.; Siegler, M. A.; Bouwman, E. Dinuclear Nickel Complexes of Thiolate-Functionalized Carbene Ligands and Their Electrochemical Properties. *Organometallics* **2018**, *37*, 740−747.
(55) Yao, S. A.; Martin-Diaconescu, V.; Infante, I.; Lancaster, K. M.; Götz, A. W.; DeBeer, S.; Berry, J. F. Electronic Structure of Ni_2E_2 Complexes (E = S, Se, Te) and a Global Analysis of M_2E_2 Compounds: A Case for Quantized E_2^{n-} Oxidation Levels with n = 2, 3, or 4. *J. Am. Chem. Soc.* **2015**, *137*, 4993−5011.
(56) Eberhardt, N. A.; Guan, H. Nickel Hydride Complexes. *Chem. Rev.* **2016**, *116*, 8373−8426.
(57) Song, L.-C.; Wang, Y.-X.; Xing, X.-K.; Ding, S.-D.; Zhang, L.-D.; Wang, X.-Y.; Zhang, H.-T. Hydrophilic Quaternary Ammonium-Group-Containing [FeFe]-Hydrogenase Models: Synthesis, Structures, and Electrocatalytic Hydrogen Production. *Chem. - Eur. J.* **2016**, *22*, 16304−16314.
(58) Bard, A. J.; Faulkner, L. R. *Electrochemical Methods: Fundamentals and Applications*, 2nd ed.; Wiley: Hoboken, NJ, 2001.
(59) Felton, G. A. N.; Glass, R. S.; Lichtenberger, D. L.; Evans, D. H. Iron-Only Hydrogenase Mimics. Thermodynamic Aspects of the Use of Electrochemistry to Evaluate Catalytic Efficiency for Hydrogen Generation. *Inorg. Chem.* **2006**, *45*, 9181−9184.
(60) Rountree, E. S.; McCarthy, B. D.; Eisenhart, T. T.; Dempsey, J. L. Evaluation of Homogeneous Electrocatalysts by Cyclic Voltammetry. *Inorg. Chem.* **2014**, *53*, 9983−10002.
(61) Borg, S. J.; Behrsing, T.; Best, S. P.; Razavet, M.; Liu, X.; Pickett, C. J. Electron Transfer at a Dithiolate-Bridged Diiron Assembly: Electrocatalytic Hydrogen Evolution. *J. Am. Chem. Soc.* **2004**, *126*, 16988−16999.
(62) Song, L.-C.; Han, X.-F.; Chen, W.; Li, J.-P.; Wang, X.-Y. Dithiolato- and halogenido-bridged nickel-iron complexes related to the active site of [NiFe]-H_2 ases: preparation, structures, and electrocatalytic H_2 production. *Dalton Trans.* **2017**, *46*, 10003−10013.
(63) Dong, W.; Wang, M.; Liu, T.; Liu, X.; Jin, K.; Sun, L. Preparation, structures and electrochemical property of phosphine substituted diiron azadithiolates relevant to the active site of Fe-only hydrogenases. *J. Inorg. Biochem.* **2007**, *101*, 506−513.
(64) Kilgore, U. J.; Roberts, J. A. S.; Pool, D. H.; Appel, A. M.; Stewart, M. P.; DuBois, M. R.; Dougherty, W. G.; Kassel, W. S.; Bullock, R. M.; DuBois, D. L. $[Ni(P^{Ph}{}_2N^{C6H4X}{}_2)_2]^{2+}$ Complexes as Electrocatalysts for H_2 Production: Effect of Substituents, Acids, and Water on Catalytic Rates. *J. Am. Chem. Soc.* **2011**, *133*, 5861−5872.
(65) Felton, G. A. N.; Mebi, C. A.; Petro, B. J.; Vannucci, A. K.; Evans, D. H.; Glass, R. S.; Lichtenberger, D. L. Review of electrochemical studies of complexes containing the Fe_2S_2 core characteristic of [FeFe]-Hydrogenase including catalysis by these complexes of the reduction of acids to form dihydrogen. *J. Organomet. Chem.* **2009**, *694*, 2681−2699.
(66) Weber, K.; Krämer, T.; Shafaat, H. S.; Weyhermüller, T.; Bill, E.; van Gastel, M.; Neese, F.; Lubitz, W. A Functional [NiFe]-Hydrogenase Model Compound That Undergoes Biologically Relevant Reversible Thiolate Protonation. *J. Am. Chem. Soc.* **2012**, *134*, 20745−20755.
(67) Song, L.-C.; Cao, M.; Wang, Y.-X. Novel reactions of homodinuclear Ni_2 complexes $[Ni(RN_{Py}S_4)]_2$ with $Fe_3(CO)_{12}$ to give heterotrinuclear $NiFe_2$ and mononuclear Fe complexes relevant to [NiFe]- and [Fe]-hydrogenases. *Dalton Trans.* **2015**, *44*, 6797−6808.
(68) Bomfim, J. A. S.; de Souza, F. P.; Filgueiras, C. A. L.; de Sousa, A. G.; Gambardella, M. T. P. Diphosphine complexes of nickel: analogies in molecular structures and variety in crystalline arrangement. *Polyhedron* **2003**, *22*, 1567−1573.
(69) *CrystalClear and Crystal Structure*; Rigaku and Rigaku Americas: The Woodlands, TX, 2007.
(70) (a) Sheldrick, G. M. *SHELXS97, A Program for Crystal Structure Solution*; University of Göttingen: Göttingen, Germany, 1997. (b) Sheldrick, G. M. A short history of SHELX. *Acta Crystallogr., Sect. A: Found. Crystallogr.* **2008**, *64*, 112−122.
(71) Sheldrick, G. M. SHELXT-Integrated space-group and crystal-structure determination. *Acta Crystallogr., Sect. A: Found. Adv.* **2015**, *71*, 3−8.